https://doi.org/10.15407/knit2024.02.093
UDC 551.510.42

I. I. SYNIAVSKYI[1], Head of Department, Candidate of Technical Sciences, Senior researcher
A. J. CASTRO-TIRADO[2], Profesores de Investigación, Ph.D. in Physics
Yu. S. IVANOV[1], Senior researcher
S. S. GUZIY[2,3], Doctor Contratado[2], Associate Professor[3], Candidate of Physical and Mathematical Sciences
Ye. A. OBEREMOK[1,4], Researcher[1], Associate Professor[4], Candidate of Physical and Mathematical Sciences

[1] Main Astronomical Observatory of the National Academy of Sciences of Ukraine
27, Akademika Zabolotnoho Str., Kyiv, 03143 Ukraine
[2] Instituto de Astrofísica de Andalucía (IAA-CSIC)
Glorieta de la Astronomía s/n, 18008 Granada, Spain
[3] Petro Mohyla Black Sea National University
10, 68 Desantnykiv Str., Mykolajiv, 54000 Ukraine
[4] Taras Shevchenko National University of Kyiv
60, Volodymyrska Str., Kyiv, 01033 Ukraine

A WIDE-ANGLE STOKES POLARIMETER FOR THE BOOTES GLOBAL TELESCOPE NETWORK. OPTICAL AND MECHANICAL DESIGN

We describe the imaging polarimeter EDIPO (Efficient & Dedicated wide-field Imaging Polarimeter) as a part of astronomical telescopes of the BOOTES (Burst Observer and Optical Transient Exploring System) network that is intended for the study of polarization features of the rapid processes of the gamma-ray bursts afterglow (Gamma-ray burst — GRB). The design of the polarimeter allows one to be installed on the network telescopes with a diameter of the main mirror up to 1.4 m. The EDIPO is designed to analyze the polarization parameters of linearly polarized light in the spectral range of 450—1000 nm. The polarization analyzer of the polarimeter does not contain moving elements and allows measurements of Stokes parameters I, Q, U of light in a 30'× 30' field of view simultaneously for one spectral band of the working spectral range. The optical part of the polarimeter was assembled and tested on a telescope with a mirror diameter of 1.2 m. The calibration approaches for the polarimeter-telescope system are considered.

Keywords: *polarization, Stokes-polarimeter, astronomical observations.*

1. INTRODUCTION

Today, the study of celestial bodies is increasingly carried out by analyzing the polarization of their own or scattered radiation. Such studies provide insight into various astrophysical events: objects of the Solar System, stellar physics, our Galaxy and the interstellar medium, extragalactic astronomy, and cosmology. In the physics of the Solar System, polarimetric observations of solar radiation scattered by asteroids allow determining their albedo and size distributions [13, 49, 60]. Measuring the polarization of light scattered by comets helps in their classification [18—20, 23]. In the context of studying the structure of our galaxy, it is expected that polarimetric measurements will allow us to map the distribution of its magnetic field lines through giant molecular clouds, provid-

Цитування: Syniavskyi I. I., Castro-Tirado A. J., Ivanov Yu. S., Guziy S. S., Oberemok Ye. A. A wide-angle Stokes polarimeter for the BOOTES global telescope network. Optical and mechanical design. *Space Science and Technology.* 2024. **30**, № 2 (147). P. 93—108. https://doi.org/10.15407/knit2024.02.093

ing an understanding of the connection of the field with the diffuse interstellar medium, which includes clouds, spheres, open clusters, etc. [12, 24, 31, 52]. In extragalactic astronomy, the sources of high-energy gamma radiation are of interest [15, 55], which are studied, for example, at the Compton Gamma-Ray Observatory (CGRO) using the Energetic Gamma-Ray Experiment Telescope (EGRET) [46]. During these studies, many blazars were discovered [2], which have an impact on the identification of most gamma-ray sources, but that still remain unknown due to large errors [48]. Gamma radiation polarization analysis will also reduce these errors. The analysis of the polarization of scattered radiation would allow us to determine some large-scale structures of the magnetic field, such as the structures of the Magellanic clouds and their relations with gas dynamics [27]. In cosmology, sampling the polarization of starlight across the sky will allow a better simulation of the polarization of the foreground galaxy at far-IR ranges and wavelengths less than 1 mm [29, 33—35, 56, 61]. Early optical polarization measurements of gamma-ray bursts (Gamma-ray burst — GRB) are very important in modern astronomy. This is due to the fact that the spectra and light curves of the GRB afterglow correspond to the model of synchrotron radiation, which is strongly polarized (up to 70 %) in a wide frequency range, which has been verified in many astrophysical cases [15, 25, 55]. The polarization of the GRB afterglow in the optical range is small (rarely more than 2 %), and theories of the origin of the optical afterglow must account for this. Although localized areas may have strong magnetic fields and high polarization, the net polarization is small unless the fields are globally aligned. Theoretical estimates predict that early long-lasting GRB afterglows should be polarized up to 3—15 % on time segments (<0.1 days) [45]. However, such early measurements are still lacking, which makes it difficult to verify theoretical estimates.

The first attempts at optical polarization studies in wide star fields were made in 1993 using wide-format Schmidt plates and polarizing films. It aimed to search for blazars on 560 square degrees of the celestial sphere [21, 53, 63]. Determining the polarization of the optical radiation of celestial bodies throughout the entire sphere has not yet been thoroughly done and remains relevant. Such problems in astrophysics can be solved with high resolution by modern robotic observation technologies in combination with the use of new matrix detectors of optical radiation. Robotic telescopes, in particular, are ideal for long-term studies and observations of fast-moving processes on astrophysical objects.

Research of the GRB, which has the highest energy levels in the Universe after the Big Bang [14], both in the optical and IR ranges, is one of the task lists of the BOOTES network (Burst Observer and Optical Transient Exploring System) [6, 7]. The BOOTES's main scientific object is the observation of the sky in real time. Polarimetric observations of GRB afterglows are planned to be carried out using polarimeters installed on robotic telescopes of the BOOTES network. The structure, principle of operation, and some test results of the EDIPO (Efficient & Dedicated wide-field Imaging Polarimeter) polarimeter are described in the following sections.

2. PRELIMINARY POLARIMETER REQUIREMENTS

Telescopes of the BOOTES network are independent functional robotic instruments for astronomical observations, thus their design does not provide the use of polarizing elements. Polarization measurements are possible only with the use of an external polarimeter which mechanical and optical parameters are matched with the corresponding parameters of a

Table 1. **Main parameters of the telescope-polarimeter system**

Parameter	Value
Telescope	Cassegrain with equatorial mounting
Diameter of the main mirror, m	1.4
Effective focal length of the telescope + polarimeter system, mm	4480
Polarimeter numerical aperture F#	3.2
Detector size, in pixels	4000 × 4000
Pixel size, mm	10 ×10
Field of view of the telescope-polarimeter system, arcmin	30 × 30
Image scale, arcsec/pixel	0.44
Spectral range, nm	450—1000
Filters	*V*, *R*, *I* (*r*, *i*, *z*)
Focusing system	Telescope secondary mirror

specific telescope. The EDIPO polarimeter considered in this paper was designed for a telescope with a diameter of the main mirror of 1.4 m and a focal length of 11.2 m. The design of the telescope and its parameters determine the main requirements for the characteristics of the telescope-polarimeter system, which are presented in Table 1.

The ordinary value of the degree of polarization of the observed celestial objects is 2 %. To achieve a polarimetric accuracy of 1 % when observing weak sources, for example, with $R = 18$, the signal/noise ratio in the polarimeter should be at least $S/N = 141$, with a single exposure of 180 seconds. With this exposure, including calibration frames, that take up to 10 % of the whole observation time, 24 square degrees of the celestial hemisphere will be surveyed during an ordinary night of 9 hours. A complete survey of the celestial hemisphere (20 000 square degrees) should be carried out in 5 years, taking into account the days with adverse weather conditions for the observation, the technical simplicity of the equipment, and the duration of the optical transients of the afterglow after the GRB. Based on the polarization measurements, it is planned to select candidates for further studies to obtain different colors and search for optical variability using the Global BOOTES network robotic telescopes [6].

3. CONCEPT OF MEASUREMENTS AND POLARIMETER OPTICAL LAYOUT

3.1. ***Choose the polarimeter measuring scheme.*** The design and parameters of the telescope optical system and the specifics of the tasks to be solved (polarization studies of fast-moving processes in several spectral ranges) determined the choice of the polarimeter measurement layout and the concept of designing its optical system. In particular, the measuring part of the EDIPO is based on the approach with the division of the amplitude or aperture (Division of Amplitude/Aperture — DoA) [22, 26, 36—39, 42, 50, 65]. According to the DoA approach, the input beam is divided into several equivalent parts that form spatially separated optical channels. In each channel, the beam passes/reflects through fixed polarizing elements (polarizers, phase plates) before entering the photodetector. In such a schematic implementation, there are no moving elements (at least within one spectral channel), and the registration of all values that are necessary for the complete characterization of the light polarization is being made in one exposure. This makes it possible to analyze the state of light polarization of fast-moving processes occurring on celestial bodies and in interstellar space. Besides all, the EDIPO is an imaging polarimeter that should allow observing the distribution of polarization over the field of view of the corresponding telescope.

3.2. ***Description of polarized light and detailing of the EDIPO measurement scheme.*** For a complete description of light with a certain wavelength with an arbitrary state of polarization, it is convenient to use the Stokes parameters I, Q, U, and V [9, 10]. They can be used to describe the degree of polarization DoP (Degree of Polarization), the azimuth of polarization AoP (Azimuth of polarization), and the angle of ellipticity EoP (Ellipticity of Polarization) of the radiation polarization ellipse:

$$\begin{aligned} \mathrm{DoP} &= \sqrt{Q^2 + U^2 + V^2}\,/\,I\,, \\ \mathrm{AoP} &= \frac{1}{2}\mathrm{arctg}\left(U/Q\right), \\ \mathrm{EoP} &= \frac{1}{2}\mathrm{arctg}\left(V/\sqrt{Q^2+U^2}\right). \end{aligned} \qquad (1)$$

The first Stokes parameter I corresponds to the total radiation intensity. Parameters Q and U determine the predominance of the linearly polarized component in the beam with polarization azimuth 0°, 90°, 45°, and 135°. The parameter V — determines the predominance of components with left or right circular polarization.

The star's light, as well as the light of other emitting celestial bodies, is mostly unpolarized, but due to the scattering of this light by gases, dust, and the surface of celestial bodies, it can acquire partial linear polarization. Therefore, most astronomical polarimeters are focused on the exact determination of the parameters of linear polarization, in particular, the degree of linear polarization (Degree of Linear Polarization — DoLP) and azimuth of linear polarization (Angle of Lineart Polarization — AoLP).

The polarization of GRB afterglows is also linear with a different degree and azimuth of polarization. Therefore, when designing EDIPO, emphasis was placed on the accurate determination of the linearly

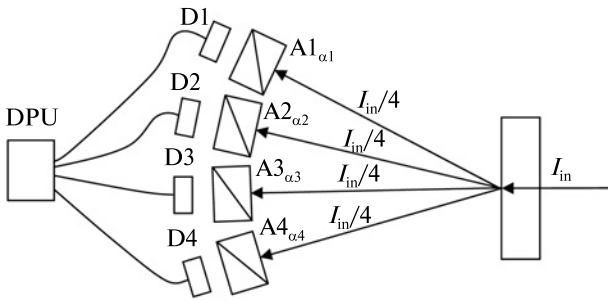

Figure 1. Scheme of a polarimeter with divided of intensity/aperture for measuring the parameters of linearly polarized radiation: I_{in} — the intensity of the incoming beam, An_{an} — linear analyzer (polarizer) of the *n*-th channel with azimuth αn, *Dn* — photodetector in the *n*-th channel, DPU (Data Processing Unit) is a data collection and processing unit

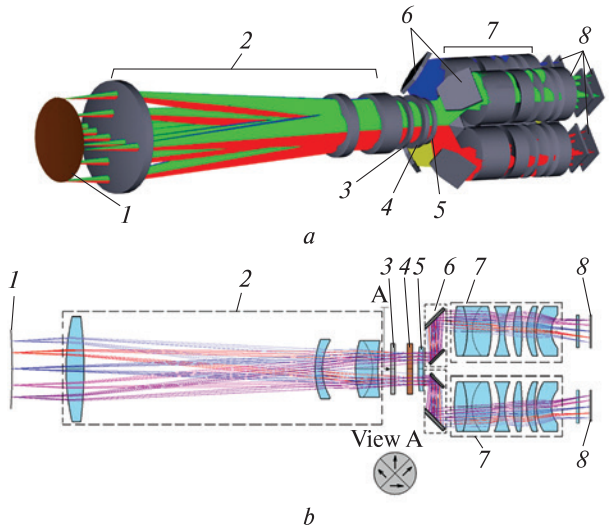

Figure 2. EDIPO polarimeter optical layout model (*a*) and its sectional view (*b*). Two polarization channels 0° and 90° are shown: *1* — telescope focal plane, *2* — collimator, *3* — polarization analyzer, *4* — spectral filter, *5* — field lens, *6* — mirror division system, *7* — camera lenses, *8* — detectors

polarized light parameters. For a complete description of linearly polarized light, the first three Stokes parameters are sufficient. They make it possible to characterize the intensity of light *I*, the degree of DoLP, and the azimuth of AoLP polarization [9]:

$$\text{DoLP} = \sqrt{Q^2 + U^2}\,/\,I\,,$$
$$\text{AoLP} = \frac{1}{2}\text{arctg}\left(U\,/\,Q\right). \qquad (2)$$

To determine Stokes parameters in DoA polarimeters, a common approach that is schematically depicted in (Fig. 1), is used. The polarimeter's separation system divides its aperture into four equivalent parts, forming four independent spatial optical channels. In each channel, the beam, before entering the photodetector, passes through an analyzer (a linear polarizer with a fixed azimuth). It is common to orient the azimuths of the analyzers in the optical channels at the angles $\alpha = 0°, 90°, 45,°$ and 135°. Then, the Stokes parameters of light at the input of the polarimeter are calculated as:

$$I = I_0 + I_{90} = I_{45} + I_{135};$$
$$Q = I_0 - I_{90};\;\; U = I_{45} - I_{135}, \qquad (3)$$

where I_0, I_{90}, I_{45}, I_{135} — light intensity at the analyzer output with the corresponding azimuth.

3.3. ***The EDIPO polarimeter optical layout model.*** The EDIPO optical layout is shown in Figure 2, *a*, and its cross-section is in Figure 2, *b*. It allows the implementation of the described measuring scheme (Fig. 1). In Figure 2, the image of the observed object (field) is formed in the focal plane of the telescope. The collimator of the polarimeter forms an image of the telescope's entrance pupil and directs it through a combined polarization analyzer (a set of linear polarizers with the required orientation) and a spectral filter to the pupil division system. The polarization analyzer shown in Fig. 2, *b* is divided into four segments of equal size. It is placed in front of the mirror division system, but, in fact, it already divides the focal plane into four parts, each of which passes through a polarizing element (a sequence of elements). Next, the mirror division system spatially divides the parts, which are then focused on the detectors by four camera lenses. To determine the parameters of linear polarization, a linear polarizer with the required orientation of the transmission axis or an equivalent system of polarization converters (prisms, films, plates) must be installed in each segment of the analyzer in Fig. 2, *b*. If it is necessary to measure full light polarization parameters, additional waveplates can be installed in the analyzer sectors of Fig. 2, *b*. The intensity of the split light is registered by the detectors. It is used to calculate the Stokes parameters using equation (3).

3.4. ***Detailing the design and parameters of EDIPO optical elements.*** The structural and optical param-

eters of the telescope (Table 1) and the tasks to be solved are mentioned above, specifying the structure of the optical system and the parameters of the polarimeter elements. The key parameters of the EDIPO optical system are listed in Table 2.

A detailed description, purpose, and possible implementation of elements of the EDIPO's optical system are given below.

The polarimeter collimator consists of four spherical lenses. The linear field of view of the collimator is 97 × 97 mm. It forms an image of the telescope's main mirror (pupil) with 60 mm diameter. The effective focal length of the collimator is 455 mm, the total length is 550 mm.

Spectral filters. To provide multispectral polarimetric measurements in the range of 450—1000 nm, the replaceable spectral filters *V, R, I* (*r, i, z*) are supposed.

Polarization analyzer. High-quality optical polarization analyzers are based on birefringent prisms [1, 11, 42]. The possible design of combined segmented prism analyzers of the type shown in Fig. 2, *b* is described in [13, 22]. Thus, in [40], this analyzer is built based on the use of a pair of two-beam Wollaston polarizing prisms, the optical axes of which are oriented at an angle of 45° to each other, and the prisms themselves fill sectors 1-2 and 3-4, respectively, and have an efficiency equal to 100 %. In [40], a double wedge

Table 2. **EDIPO optical system parameters**

Parameter	Value
Spectral range, nm	450—1000
Camera lens aperture ratio D/f	1/3.2
Collimator diameter, mm max/min	160/84
Collimator length, mm	600
Number of collimator lenses	4
Camera lens length, mm	160
Camera lens diameter, mm	76
Number of camera lens lenses	7
Polarimeter pupil diameter, mm	60
Mirror division system diameter, mm	180
Number of detectors,	4
Detector size, pixels	4000 × 4000
Pixel size, mm	10
Polarimeter aperture ratio D/f	3.2

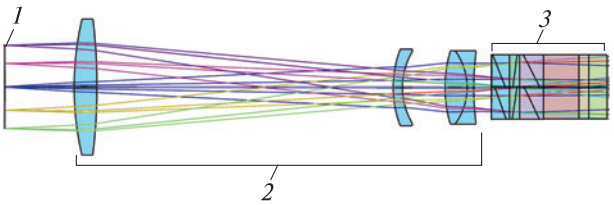

Figure 3. Ray's propagation in the part of polarimeter optical system collimator — polarization analyzer for option the analyzer based of achromatized Wollaston prisms: *1* — telescope focal plane, *2* — collimator, *3* — double Wollaston prism

Wollaston prism was proposed to determine the first three Stokes parameters of linearly polarized light. In [39, 43, 47, 51], in addition to the array of Wollaston prisms, a quarter wave plate is also used as a polarization analyzer to determine all Stokes parameters. However, the own dispersion of the prisms requires the use of additional compensation wedges. The [28] presents the development of a polarimeter based on pairs of Wollaston prisms, which use a system of wedges for dispersion compensation.

The advantage of using polarizing prisms based on birefringent crystals is the highest polarization contrast (extinction ratio) ($1{:}10^5$...$1{:}10^6$) and the lowest absorption in a wide range of wavelengths (300—2500 nm) compared to other types of linear polarizers.

Thus, the use of polarizing prisms for the design of the segmented polarizer EDIPO (Fig. 2, *b*) was also considered. In particular, the optical system of the polarimeter was modeled, where the analyzer is built on the basis of a pair of Wollaston prisms. The optical axes are at an angle of 45° relative to each other. One of the disadvantages of Wollaston prisms is the dependence of the angle between the ordinary and extraordinary output rays on the wavelength of the input light. Simulation shows that achromatization of the Wollaston prism in the spectral range of EDIPO operation (450—1000 nm) is possible. For that purpose, one should be three-component. It is also necessary to use additional compensating prisms, which should include at least 3 wedges. The path of rays in the optical system of the polarimeter in the collimator-analyzer part, if the design of the analyzer is based on achromatic Wollaston prisms, is presented in Fig. 3.

Figure 4 show the structure and dimensions of the analyzer unit based on two Wollaston prisms with

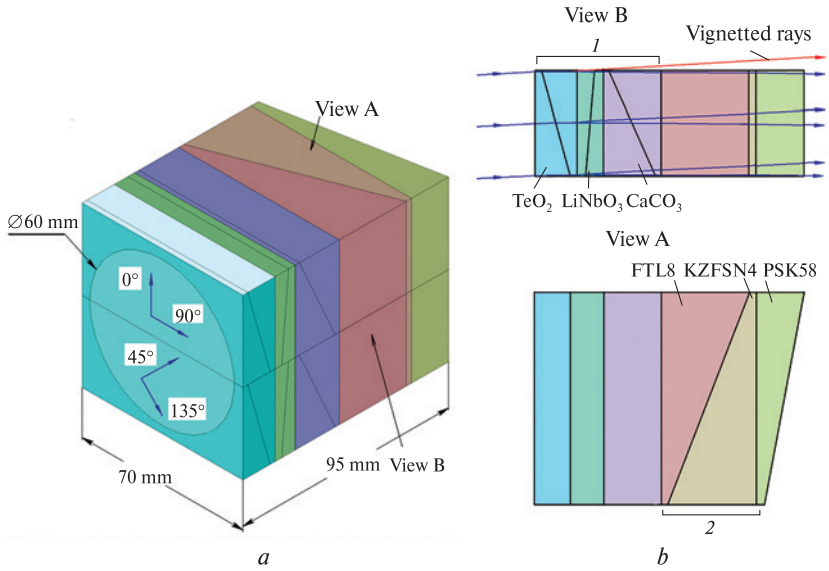

Figure 4. General view of the of Wollaston prisms unit with compensating wedges (a) and composition of one Wollaston prism with compensation wedges (*b*). B — side view, A — top view

compensating wedges. Figure 4, *a* shows the general view of the analyzer, and Figure 4, *b* shows the appearance and composition of one of its prisms. The appropriate combination of birefringent crystals and crystals is $CaCO_3$ + $LiNbO_3$ + TeO_2. This combination, together with the PSK58 + KZFSN4 + FTL8 (Schott and Ohara) glass apochromatic wedge system, can deflect light beams at angles up to 6° and forms two channels (camera lens, detector) for analyzing the polarized light parameters.

With a light diameter of 60 mm, the total thickness of the analyzer unit in Fig. 4, *a* should be 95 mm. The analyzer in Fig. 4, *a* is equivalent to the segmented analyzer in Fig. 2, *b*. Each prism of the block in Fig. 4, *a* forms two adjacent segments of the analyzer in Fig. 2, *b* (1-2 and 3-4).

The main disadvantages of the considered analyzer are:

— large dimensions,

— vignetting of rays at the edge of two adjacent Wollaston prisms (for edge rays can be up to 20—25 %),

— different dispersion of Wollaston prisms for two orthogonal directions of light propagation, as a result of which the images of the object constructed by camera lenses are not identical.

The analysis showed that it would be technologically difficult to ensure the necessary homogeneity and uniformity of Wollaston prism parameters within the light beam diameter of 60 mm and wavelength range of 400—1000 nm. The errors caused by these imperfections will be difficult to account for and will greatly complicate the calibration procedure. Furthermore, it is expected the described assemble would be too expensive. Therefore, the use of considered prism analyzers is impractical.

As an alternative way, the design of a segmented analyzer based on polarization cubes with a polarization multilayer coating was also analyzed [44]. The design of the segmented analyzer proposed by the authors is presented in Fig. 5. As can be seen, the specified system is cumbersome and structurally complex. The main advantage of using polarization cubes is their relatively low cost compared to Wollaston prisms. At the same time, the cubes have a selective transmittance and cannot cover wide spectral ranges. On the other hand, the complexity of assemble configuration Fig. 5 precludes a quick change of cubes for different ranges, which also makes this solution unsuitable for use in EDIPO.

The use of polarizing films simplifies the design of the segmented analyzer significantly. All we have to

do is place polarizing films with a given azimuth of the transmission axis in the corresponding segments of the analyzer (Fig. 2, *b*). The polarization analyzer commonly installed in the image plane of the entrance pupil (main mirror of the telescope), which is formed by a system of parallel rays, with angles of incidence different from 0°. The actual value of the incidence rays' angle on the segments of the analyzer, on the one side, is determined by the constructive displacement of the segments relative to the optical axis of the polarimeter, on the other side, by the actual field of view (FOV) of the telescope.

With a wide FOV, vignetting of oblique field rays occurs at the edges of contact of the analyzer segments. The thicker the polarization analyzer, the greater the vignetting (see Fig. 4, *b*). The use of films minimizes the thickness of the analyzer and, accordingly, additional vignetting since the range of permissible input angles of polarizing films is tens of degrees, which is an order more than available for prism polarizers and polarizing cubes.

The disadvantage of polarizing films, operating in a wide spectral range, for example, 400—700 nm, is relatively low transmittance (actually below 47 %) and relatively low polarization contrast that does not exceed $1{:}10^4$ [https://www.edmundoptics.com/f/high-contrast-linear-polarizing-film/14385/]. However, polarizing films, operating in narrow spectral ranges, have a polarization contrast greater than $1{:}10^4$ and a transmittance of 60—80 %. The use of a set of narrow-band polarization films for several wavelength ranges will allow covering the spectral range of 450—1000 nm [https://www.codixx.de/en/colorpolr-polarisationen/uv-polarisatoren]. A significant advantage of using the polarizing films-based segmented analyzers is the simplicity of replacing analyzers simultaneously with a spectral filter when changing the desired spectral range during the observation process.

Taking into account the disadvantages and advantages of the considered different implementations of segmented polarization analyzer, the EDIPO analyzer was designed with the use of codixx VIS 500 BC4 and VIS 700 BC4 polarization films, which overlap the spectral range 550—1100 nm.

The field lens (Fig. 1, 2) has a low optical power of $1/f \approx 1.7 \quad 10^{-3}$ m^{-1} and is installed in front of

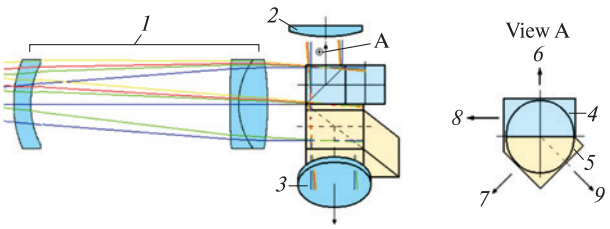

Figure 5. Segmented polarization analyzer based on polarization cubes: *1* — collimator, *2* — camera lens 0°, *3* — camera lens 45°, *4* — polarizing cube 0°—90°, *5* — polarizing cube 45°—135°, *6* — to camera lens 0°, *7* — to camera lens 45°, *8* — to camera lens 90°, 9 — to camera lens 135°

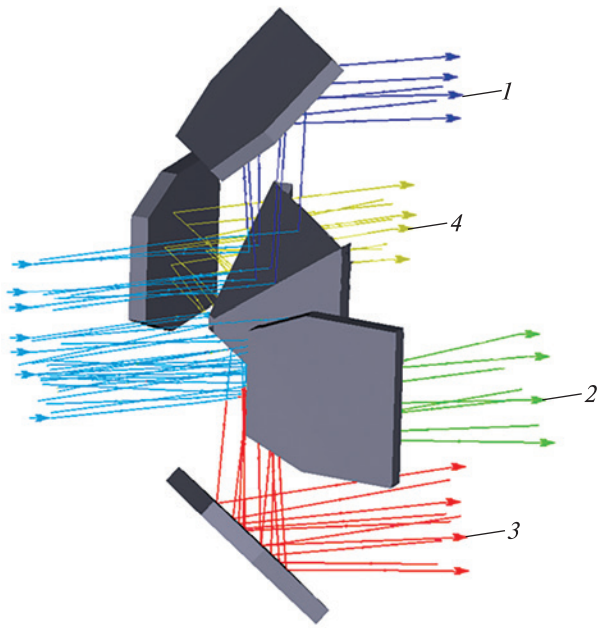

Figure 6. Mirror division system: *1* — to camera lens 0°, *2* — to camera lens 45°, *3* — to camera lens 90°, *4* — to camera lens 135°

the mirror division system. It is intended to reduce the diameter of the off-axis beams, which are then spread in the optical system.

Mirror division system. The polarimeter has a mirror division system for the spatial division of input light parts that have passed through the corresponding segments of the analyzer. It consists of a pyramid with four reflective faces and four mirrors (Fig. 6). Each pyramid surface is positioned to reflect part of the light that has passed through a certain segment of the analyzer onto one of the mirrors. Next, the di-

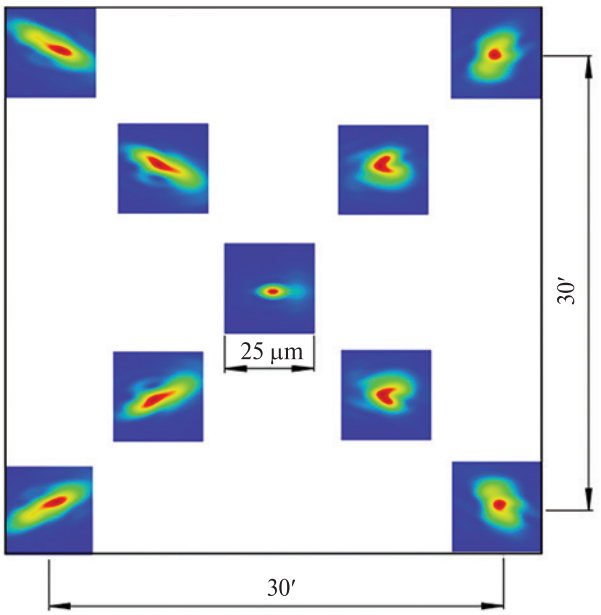

Figure 7. Model spot diagrams (artificial star) in the focal plane of a camera lens

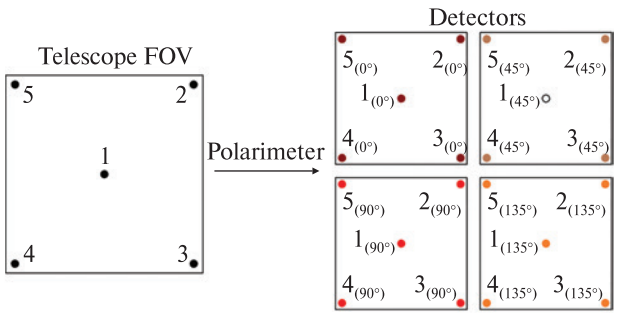

Figure 8. Forming of the input field image on EDIPO matrix detectors

vided rays are directed by mirrors into four camera lenses. In this way, four spatially divided channels are obtained, and the light of each is registered by the detector. This mirror system does not have chromatic aberrations, unlike, for example, the wedge system [54, 57, 58], and its location after the analyzer (along the path of light propagation) does not affect the determination of the input light polarization parameters. The contribution of the system to the effective values of the transmission coefficients of the polarimeter channels will be automatically taken into account during calibration.

Camera lenses. The general view of the camera lens optical system is shown in Fig. 2, *a*. Each camera lens consists of a triplet and four single lenses. The focal length of the lens is 225 mm, the maximum light diameter of lenses is 76 mm. After passing through the mirror division system, ¼ of the total light goes to each camera lens. At the same time, the light diameters have an asymmetric shape, and therefore, asymmetric spots are formed in the camera lenses' focal planes. In Fig. 7, the model spot diagrams (artificial star), which are formed by the polarimeter optical system in the focal plane of one of the four camera lenses, are presented. Spots are modeled for different coordinates of the FOV (center, middle, edge). The scale of the figure is 30′, which corresponds to the telescope FOV. In Fig. 7, the scale of spots has been increased to better illustrate the distribution of asymmetry along the plane of the detector. As shown in Fig. 7, the difference in the spot size in the center and on the corner does not exceed 1 pixel (10 μm) in the focal plane of the camera lens.

Detectors. A matrix detector is placed in the focal plane of each of the four camera lenses. Schematically, the correspondence of the points on the polarimeter matrix detector to the points of the input field of the polarimeter is shown in Fig. 8. In the right part of the figure, the numbers in brackets indicate which segment of the analyzer this spatial channel corresponds to. The asymmetry of the shape of the light rays in the camera lenses leads to different asymmetry of the spots in the corresponding spatial channels of the polarimeter, which can be compensated for by geometrical calibration of the polarimeter.

4. POLARIMETER MECHANICAL DESIGN

Details and features of the EDIPO polarimeter design, which implements the concept discussed in the previous section, are given below.

The design simulation of the instrument is shown in Fig. 9. The polarimeter consists of the units: the collimator unit *1*, the unit of polarizers and spectral filters *2*, the mirror division system unit *3*, the camera lens unit *4*, and the matrix detector.

The front part of the polarimeter contains a collimator tube, which consists of two parts. The first collimator lens is installed in the first part of the tube. The rear part of the tube is centered and attached to

the unit of polarizers and spectral filters. Structurally, other collimator lenses are attached to the unit of polarizers and spectral filters. The tolerance for centering the collimator lenses is 0.1 mm and is fully achievable in the design.

The unit of polarizers and spectral filters is a composite frame. It has three wheels which have 6 positions each. The main wheel is for polarizers, the others are for spectral selection elements (spectral filters, transmissive diffraction gratings). Changing the elements' position in each wheel is carried out using stepper motors. A field lens is coaxial with the optical axis of the collimator, and it is also attached to the unit. A collimator is attached to the unit's front part, and the mirror division system is attached to the unit's rear part.

The model of the mirror division system unit in section 3/4 is presented in Fig. 10, *a*. The elements of the system are a mirror pyramid, which consists of four separate mirrors glued to an aluminum pyramid, four units of diagonal mirrors, and a frame. The design includes a system of adjusting screws. The additional baffles are provided between adjacent mirror faces in the mirror pyramid to block the stray light.

The camera lens unit is presented in Fig. 10, *b*. It consists of four lenses of the same type placed in a housing. The design allows you to focus each lens separately during adjustment and adjust the unit as a whole. The camera lens unit is connected to the mirror division system unit by the flange of the left part (relative to the ray propagation). The unit is connected to the detector with the right flange.

5. ADJUSTMENT AND PRELIMINARY EXPERIMENTAL RESULTS

Simulation of the errors in the alignment of optical elements of the polarimeter has provided to separate the most critical of them. As a result, the permissible deviations of the design parameters and spatial positions of these optical elements were determined. The most stringent requirements are defined for the spatial placement of the mirrors of the division system and the relative placement of the camera lens lenses. The error in the spatial arrangement of the faces of the monolithic pyramid and the fold mirrors of the division system is <3 arcsec, and the error in the relative location of the lenses of the camera lenses is <0.1 mm.

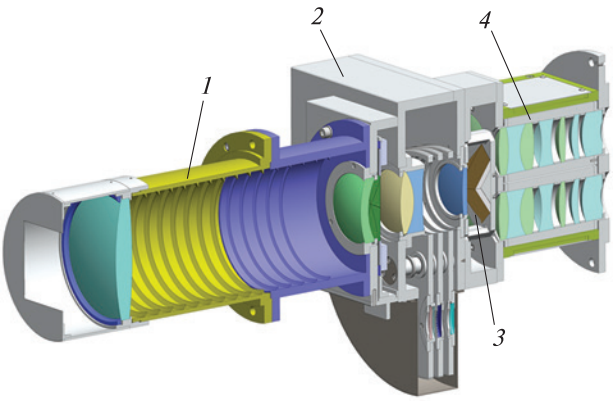

Figure 9. Design simulation of the EDIPO polarimeter: *1* — collimator unit, *2* — unit of polarizers and spectral filters, *3* — mirror division system unit, *4* — camera lens unit

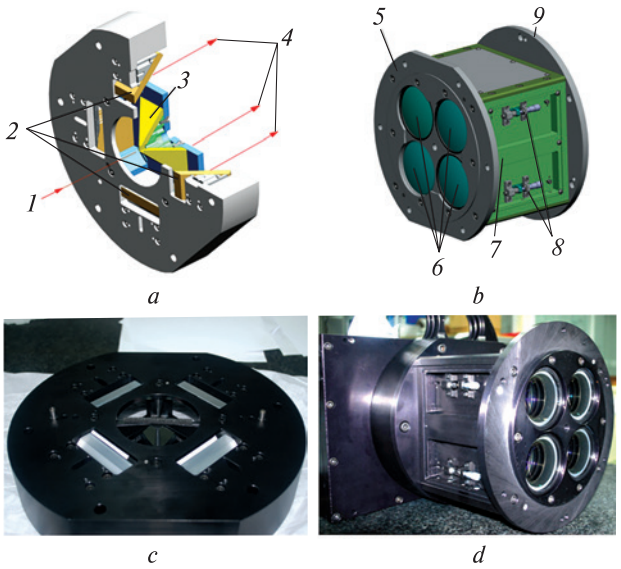

Figure 10. Mirror division system unit (*a*) and camera lenses unit (*b*) of EDIPO polarimeter and its general view (*c, d* respectively): *1* — input light, *2* — fold mirrors, *3* — mirror pyramid, *4* — output light, *5* — flange to mirror division system, *6* — camera lenses, *7* — housing, *8* — mechanism for adjustment, *9* — flange to detector

All the design elements of the EDIPO polarimeter were produced by Added Value Solutions company (AVS) https://www.a-v-s.es/. The assembly and adjustment of the polarimeter were also carried out in the optical laboratory of the company according to the correspondingly developed procedures. For the

a *b*

Figure 11. EDIPO camera and control electronics unit assembly (*a*) and general view of the assembled EDIPO polarimeter (*b*)

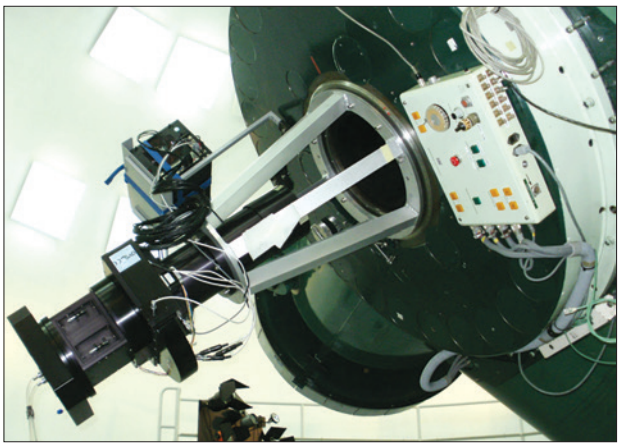

Figure 12. Stokes polarimeter EDIPO installed on the telescope of the Caral Alto Observatory

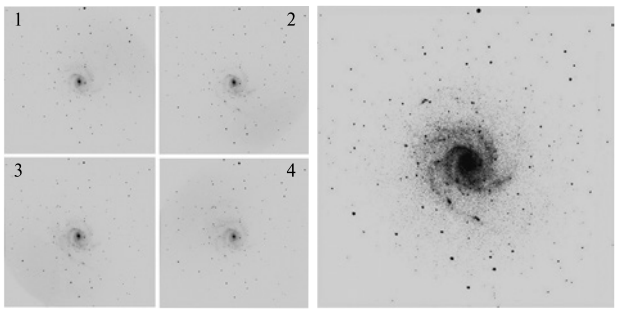

a *b*

Figure 13. Four images of the sky around galaxy M101 on polarimeter detectors 1—4 (*a*) and central part of the polarimeter's FOV, obtained as a result of the sum of this four images (*b*)

intermediate step of checking each camera lens unit, the classic method was used. The "artificial star" in the focal plane of the collimator was installed, the image of which was then analyzed by each lens. The results of testing the camera lenses showed a correlation between real and modeled image quality parameters (Fig. 7).

The spatial position of each fold mirror relative to the corresponding face mirror of the pyramid was controlled by the collimation method. This ensured the necessary accuracy in the relative location of the mirror faces of the prism and the rotating mirrors within 3 arcsec.

For the polarimeter, a camera containing four separate matrix detectors was developed (Fig. 11, *a*). The control electronics unit and detectors are made in a single housing. The size of each detector is 4000 × 4000 pixels with a pixel size of 10 μm.

The general view of the assembled EDIPO polarimeter is shown in Figure 11, *b*.

The first images on the polarimeter were obtained at the Caral Alto observatory using a telescope with a mirror diameter of 1.2 m [https://www.caha.es/CAHA/Telescopes/1.2m.html] (Fig. 12). The images of the sky were obtained without the use of polarizers. We estimated only the image quality at this stage.

Figure 13, *a* shows images of 1—4 of the polarimeter detectors when observing the area of the sky around the galaxy M101. Figure 13, *b* shows the result of the sum of images 1—4 (displays the double value of the intensity distribution through the observed scene). Figure 13, *b* shows an enlarged central part of the FOV with an image of the M101 galaxy to illustrate the resolution of the polarimeter-telescope system.

6. GEOMETRIC AND POLARIZATION CALIBRATION EDIPO

The next step to ensure the full functioning of EDIPO as a part of the telescope is the geometric and polarization calibration. In this case, the essence of geometric calibration is to estimate offsets of pixel coordinates in each of the four received images.

For this purpose, it is planned to use a laboratory calibration stand with an image of a "checkerboard" type structure [41] or chess mates [3, 64] with subsequent localization of the coordinates of the

"checkerboard" nodes on the images in the EDIPO channels. There are techniques of geometric calibration based on using reference light sources with a well-defined direction of view [4] and that utilize precise turntables [8, 17]. The final relative values of coordinate offsets in the channels will be determined by averaging the offsets obtained for the nodes of the calibration image. The maximum distortion of the EDIPO optical system is 1.2 %, so its compensation is provided according to the method proposed by the authors in [32].

Polarization imperfections of the optical system of the telescope and polarimeter (birefringence in the lenses caused by mechanical stresses in their material), errors in the orientation of the polarizing films in the analyzer segments, the finite polarization contrast of the polarizing films, the difference in the photoelectric characteristics of the detectors will increase the systematic polarimetric error of the system. The influence of these negative factors on the polarization measurements of polarimeters is usually described by the instrumental matrix [62] or instrumental polarizations [5, 13]. Determining the instrumental matrix/polarizations of the polarimeter and using it to adjust the results of subsequent measurements is the essence of polarimetric calibration.

For the polarimetric calibration of the telescope-EDIPO system, the approach described in [32, 59] can be partially used. The measurement equation of the system for each pixel of the input image has the form:

$$\begin{bmatrix} I_0 \\ I_{90} \\ I_{45} \\ I_{135} \end{bmatrix} = \underbrace{\begin{bmatrix} 1 & a_1\cos 2\varepsilon_1 & a_1\sin 2\varepsilon_1 \\ 1 & -a_2\cos 2\varepsilon_2 & -a_2\sin 2\varepsilon_2 \\ 1 & -a_3\sin 2\varepsilon_3 & a_3\cos 2\varepsilon_3 \\ 1 & a_4\sin 2\varepsilon_4 & -a_4\cos 2\varepsilon_4 \end{bmatrix}}_{\mathbf{M}_{inst}} \cdot \begin{bmatrix} I \\ Q \\ U \end{bmatrix}, \quad (4)$$

where I, Q, U — Stokes parameters for an image within a pixel, indices — 0, 90, 45, 135, indicate the corresponding spatial (polarization) channels 0°, 90°, 45°, 135°; $I_0 = ARD_0$, $I_{90} = AK_1RD_{90}$, $I_{45} = AK_2RD_{45}$, $I_{135} = AK_3RD_{135}$ — are the light intensities on the detector pixels of the corresponding spatial channel. At the same time $RD_{0,\,90,\,45,\,135} = R_{0,\,90,\,45,\,135} - D_{0,\,90,\,45,\,135}$ data from the analog-to-digital converter (ADC) of the EDIPO camera corrected for the offset of the "electrical zero", $D_{0,\,90,\,45,\,135}$ — determines the dark signal level ("electrical zero") of the detector when the EDIPO input light is blocked, A — is a radiometric coefficient for converting digital ADC values into an absolute radiometric scale, if necessary, K_1—K_3 coefficients, compensating for the difference in signals at EDIPO detectors when observing a non-polarized source, e_n — polarization contrast of polarizing films in the analyzer segments ($0^o + \varepsilon_1$, $90^o + \varepsilon_2$, $45^o + \varepsilon_3$, $135^o + \varepsilon_4$) (Fig. 2, *b*), $a_n = (e_n - 1)/(e_n + 1)$ — effective factor that takes into account the finite polarization contrast of polarizing films of the EDIPO analyzer, ε_n — effective angular errors in setting the azimuths of polarizers in the analyzer segments.

The corresponding coefficients are effective values since they take into account the effect on the polarization measurements of both the EDIPO elements and the telescope. $\mathbf{M}_{inst}$ in eq. (4) is the instrumental matrix of the telescope-EDIPO system. Note that the form of measurement equation (4) is general for all points of the input image of the system. At the same time, each point of the input image corresponds to its own numerical instrumental matrix.

Calibration procedures are described in [32], which allow determining the coefficients of the instrumental matrix in (4) at laboratory conditions. However, the use of such procedures is impossible for the telescope-EDIPO system due to the stationary placement and significant dimensions of the entire measuring system. In astronomical research, the instrumental matrix or polarization is determined using observations of standard stars with low polarization [13, 16].

When observing the source of unpolarized radiation in (4), it becomes possible to determine the values of the coefficients K_1—K_3 as:

$$K_1 = \frac{RD_{90}}{RD_0}, \quad K_2 = \frac{RD_{45}}{RD_0}, \quad K_3 = \frac{RD_{135}}{RD_0}. \quad (5)$$

It will obviously be necessary to determine the value of these coefficients for a discrete set of different angles of observation of the source and to carry out an approximation over the entire field of view based on the discrete values.

To determine the instrumental matrix $\mathbf{M}_{inst}$, it is necessary to measure the intensities in the EDIPO channels when observing three different polarization

standard stars, which have maximally different and well-known light polarization azimuths. Then, the expression for determining the instrumental matrix of the telescope-EDIPO system will have the form:

$$\mathbf{M}_{inst} = \begin{bmatrix} I_0^{(1)} & I_0^{(2)} & I_0^{(3)} \\ I_{90}^{(1)} & I_{90}^{(2)} & I_{90}^{(3)} \\ I_{45}^{(1)} & I_{45}^{(2)} & I_{45}^{(3)} \\ I_{135}^{(1)} & I_{135}^{(2)} & I_{135}^{(3)} \end{bmatrix} \begin{bmatrix} I^{(1)} & I^{(2)} & I^{(3)} \\ Q^{(1)} & Q^{(2)} & Q^{(3)} \\ U^{(1)} & U^{(2)} & U^{(3)} \end{bmatrix}^{-1}, \quad (6)$$

where the lowercase letter (m) denotes the values determined for the m-th polarization standard.

One of the advantages of the described procedure is the automatic accounting of atmospheric effects in the instrumental matrix (6), which can also lead to additional instrumental polarization in the case of the possibility of its practical implementation.

7. RESULTS AND DISCUSSION

One of the tasks of the EDIPO polarimeter design is to ensure its versatility and multifunctionality. The polarimeter should ensure the operation of the telescope in the photometric multispectral mode and the mode of polarization measurements. To ensure this functionality, the design of the polarimeter involves the installation of a unit of polarizers and spectral filters (Fig. 9). These units include three wheels with fixed spectral filters, polarization analyzers, phase plates, or a combination of them. To ensure astronomical observations, one of the wheel's hole positions can be empty or contain a fused silica window. Since the polarimeter collimator forms a system of parallel beams, only elements that work in converging beams — narrow-band interference filters and diffraction gratings — can be installed in the wheel. Any combination of filters, film polarizers, phase plates, and diffraction gratings can be inserted into the pupil sectors.

The versatility of EDIPO requires a multi-step setup and testing process. The first step, the results of which are presented above, involved the optical adjustment of EDIPO on the telescope of the Calar Alto Observatory with a main mirror diameter of 1.2 m (Fig. 12) to ensure their full compatibility, without spectral filters and polarizing elements. As a result, test observations showed that the optical aberrations of EDIPO agree with the calculated values for the four channels of the polarimeter. The difference in the geometric parameters of the images in the channels does not exceed 1 pixel.

In this way, the complete compatibility of the optical parameters of the polarimeter and the telescope was established, which allows them to be used in a complex for conducting astronomical observations. At the same time, parallel measurements in four EDIPO channels of equivalent images of objects can be used for an additional 4-fold averaging of the observed picture without increasing the exposure time.

In the next step, photometric and polarimetric calibration of EDIPO is planned following the procedure described in the previous section using celestial stellar standards.

Although the analysis of the light polarization parameters is performed simultaneously for the entire FOV in the polarimeter, to ensure multispectral measurements using EDPO in the range of 450—1000 nm, it will be necessary to change the spectral filters and polarization analyzers by rotation of the wheels. This disadvantage can be partially eliminated by using combined spectral filters or diffraction gratings as spectrally selective elements, as in the HARP case [30], for instance. However, such a decision will inevitably lead to a decrease in the resolution of the proportional to the increase in the number of simultaneously registered spectral channels.

8. CONCLUSIONS

The EDIPO imaging polarimeter was developed, intended for use in conjunction with astronomical telescopes of the BOOTES network to study the polarization features of the rapid processes of the afterglow of gamma-ray bursts (GRB).

The design of the polarimeter, optical parameters, and the choice of measurement scheme are determined by the design features of the BOOTES network telescopes and the specifics of the polarization studies. The possibility of studying polarization distributions in fast light-emitting processes is provided by a one-moment analysis of the polarization of the observed scene in four azimuthal directions of 0°, 45°, 90° and 135°.

The design of EDIPO allows it to be used as a conventional telescope registration system and as a

spectrophotometer and polarimeter after appropriate calibration. Such universality is provided by the use in the design of the polarimeter changeable wheels with elements of spectral selection and polarization analyzers.

The polarimeter was manufactured, assembled, and tested in the AVS optical laboratory. Test observations of celestial objects were carried out at the Calar Alto observatory on a telescope with a main mirror diameter of 1.2 m. Testing was carried out in non-polarization mode. The experimentally demonstrated image quality is in agreement with the theoretical assessments.

Further work involves testing the polarimeter in polarization mode using celestial polarization standards.

REFERENCES

1. Afanasiev V. L. Shablovinskaya E. S., Uklein R. I., Malygin E. A. (2021). Stokes-Polarimeter for 1-m Telescope. *Astrophys. Bull.,* **76**(1), 102—108. DOI: 10.1134/S1990341321010028.
2. Angel J. R. P., Stockman H. S. (1980). Optical and infrared polarization of active extragalactic objects. *Annu. Rev. Astron. and Astrophys.,* **18**, 321—361. DOI: 10.1146/annurev.aa.18.090180.001541
3. Bauer M., Grießbach D., Hermerschmidt A., Krüger S., Scheele M., Schischmanow A. (2008). Geometrical camera calibration with diffractive optical elements. *Opt. Express*, **16**, 20241—20248. DOI: 10.1364/OE.16.020241.
4. Bret-Dibat T., Andre Y., Laherrere J. M. (1995). Preflight calibration of the POLDER instrument. *Proc. SPIE*, **2553**, 218—231.
5. Cairns B., Russell E. E., Travis L. D. (1999). Research Scanning Polarimeter: calibration and ground-based measurements. *Proc. SPIE*, **3754**, 186—196. DOI: 10.1117/12.366329
6. Castro-Tirado A. J., Cunniffe R., de Ugarte Postigo A., Jelínek M., Vitek S., Kubánek P., Gorosabel J., Castillo Carrión S., Mateo Sanguino T. J., Riva A., Conconi P., di Caprio V., Zerbi F., Amado P., Cárdenas C., Claret A., Guziy S., Martín-Ruiz S., Sánchez M. A., García Teodoro P., Castro Cerón J. M., Díaz Verdejo J., Hudec R., López Soler J. M., Berná Galiano J. Á., Casares J., Fabregat J., Páta P., Sánchez Fernández C., Sabau-Graziati M. D., Trigo-Rodríguez J. M., Vitali F. (2006). BOOTES-IR: a robotic nIR astronomical observatory devoted to follow-up of transient phenomena. *Proc. SPIE*, **6267**, 62670I. DOI: 10.1117/12.671579.
7. Castro-Tirado A. J., Soldán J., Bernas M., Páta P., Rezek T., Hudec R., Sanguino T. M., de la Morena B., Berná J. A., Rodríguez J., Peña A., Gorosabel J., Más-Hesse J. M., Giménez A. (1999). The Burst Observer and Optical Transient Exploring System (BOOTES). *Astron. and Astrophys. Suppl. Ser.*, **138,** 583—585. DOI: 10.1051/aas:1999362.
8. Chen L. G., Zheng X. B., Hong J., Qiao Y. L., Wang Y. J. (2010). A novel method for adjusting CCD camera in geometrical calibration based on a two-dimensional turntable. *Optik*, **121**, 486—489. DOI: 10.1016/j.ijleo.2008.08.004.
9. Chipman R. A., Lam W. S. T., Young G. (2018). *Polarized Light and Optical Systems*. CRC Press, Taylor & Francis Group. Ser.: Optical Sciences and Applications of Light, 1036 p. ISBN 9781351129121. DOI: 10.1201/9781351129121.
10. Collett E. (2005). *Field Guide to Polarization*. SPIE Press, 134 p. ISBN: 9780819458681
11. Collins P., Redfern R. M., Sheeha B. (2008). Design, Construction and Calibration of the Galway Astronomical Stokes Polarimeter (GASP). *AIP Conf. Proc.*, **984**, 241—246. DOI: 10.1063/1.2896936.
12. Crutcher R. M., Wandelt B. D., Heiles C., Falgarone E., Troland T. H. (2010). Magnetic Fields in Interstellar Clouds from Zeeman Observations: Inference of Total Field Strengths by Bayeslan Analysis. *Astrophys. J.*, **725**, 466—479. DOI: 10.1088/0004-637X/725/1/466.
13. Devogèle M., Cellino A., Bagnulo S., Rivet J. P., Bendjoya P., Abe L., Pernechele C., Massone G., Vernet D., Tanga P., Dimur C. (2017). The Calern Asteroid Polarimetric Survey using the Torino polarimeter: assessment of instrument performances and first scientific results. *Mon. Notic. Roy. Astron. Soc.,* **465**, 4335—4347. DOI: 10.1093/mnras/stw2952
14. Fishman G. J., Meegan C. A. (1995). Gamma-Ray Bursts. *Annu. Rev. Astron. and Astrophys.*, **33**, 415—458. DOI: 10.1146/annurev.aa.33.090195.002215.
15. Götz D., Laurent P., Lebrun F., Daigne F., Bošnjak Ž. (2009). Variable polarization meashured in the prompt emission of GRB 041219A using IBIS on board integral. *Astrophys. J.*, **695**, L208. DOI: 10.1088/0004-637X/695/2/L208.
16. Heiles C. (2000). 9286 Stars: Anglomeration of Stellar Polarization Catalogs. *Astron. J.,* **119**(2), 923—927. DOI: 10.1086/301236
17. Huang C., Meng B., Chang Y., Chen F., Zhang M., Han L., Xiang G., Tu B., Hong J. (2020). Geometric calibration method based on a two-dimensional turntable for a directional polarimetric camera. *Appl. Opt.*, **59**(1), 226—233. DOI: 10.1364/AO.59.000226.

18. Ivanova O. V., Dlugach J. M., Afanasiev V. L., Reshetnyk V. M., Korsun P. P. (2015). CCD polarimetry of distant comets C/2010 S1 (LINEAR) and C/2010 R1 (LINEAR) at the 6-m telescope of the SAO RAS. *Planet. and Space Sci.*, **118**, 199—210. DOI: 10.1016/j.pss.2015.05.009
19. Ivanova O., Rosenbush V., Afanasiev V., Kiselev N. (2017). Polarimetry, photometry, and spectroscopy of comet C/2009 P1 (Garradd). *Icarus*, **284**, 167—182. DOI: 10.1016/j.icarus.2016.11.014.
20. Ivanova O., Rosenbush V., Luk'yanyk I., Kolokolova L., Kleshchonok V., Kiselev N., Kirk Z. R. (2021). Observations of distant comet C/2011 KP36 (Spacewatch): photometry, spectroscopy, and polarimetry. *Astron. and Astrophys.*, **651**, A29. DOI: 10.1051/0004-6361/202039668.
21. Jannuzi B. T., Green R. F., French H. (1993). An optical polarization survey for BL Lacertae objects and highly polarized quasars. *Astrophys. J.*, **404**, 100—111. DOI: 10.1086/172262
22. Kawabata K. S., Nagae O., Chiyonobu S., Tanaka H., Nakaya H., Suzuki M., Kamata Y., Miyazaki S., Hiragi K., Miyamoto H., Yamanaka M., Arai A., Yamashita T., Uemura M., Ohsugi T., Isogai M., Ishitobi Y., Sato S. (2008). Wide-field one-shot optical polarimeter: HOWPol. *Proc. SPIE*, **70144L**. DOI: 10.1117/12.788569
23. Kolokolova L., Kimura H., Kiselev N., Rosenbush V. (2007). Two different evolutionary types of comets proved by polarimetric and infrared properties of their dust. *Astron. and Astrophys.*, **463**(3), 1189—1196. DOI: 10.1051/0004-6361:20065069.
24. Li H.-B. (2021). Magnetic Fields in Molecular Clouds — Observation and Interpretation. *Galaxies*, **9**(2), 41. DOI: 10.3390/galaxies9020041
25. Lin H.-N., Li X., Chang Z. (2017). Polarization of gamma-ray burst afterglows in the synchrotron self-Compton process from a highly relativistic jet. *Chinese Phys.*, **41**(4), 045101. DOI: 10.1088/1674-1137/41/4/045101
26. Llull P., Myhre G., Pau S. (2011). Lens array Stokes imaging polarimeter. *Meas. Sci. Technol.*, **22**, 065901. DOI: 10.1088/0957-0233/22/6/065901
27. Magalhães A. M., Gomes A. L., de Almeida V. A., Rodrigues C. V., Pereyra A., Wisniewski J., Bjorkman K., Bjorkman J., Meade M., Babler B. L. (2008). The magnetic field structure of the Small Magellanic Cloud. *Proc. IAU*, **4**, S256, 178—183. DOI: 10.1017/S1743921308028421
28. Maharana S., Kypriotakis J. A., Ramaprakash A. N., Rajarshi C., Anche R. M., Shrish Shrish, Blinov D., Eriksen H. K., Ghosh T., Gjerløw E., Mandarakas N., Panopoulou G. V., Pavlidou V., Pearson T. J., Pelgrims V., Potter S. B., Readhead A. C. S., Skalidis R., Tassis K., Wehus I. K. (2021). WALOP-South: A Four Camera One Shot Imaging Polarimeter for PASIPHAE Survey. Paper I. Optical Design. *J. Astron. Telesc., Instrum., and Systems*, **7**(1), 014004. DOI: 10.1117/1.JATIS.7.1.014004.
29. Martínez-Solaeche G., Karakci A., Delabrouille J. (2018). A 3D model of polarized dust emission in the Milky Way. *Mon. Notic. Roy. Astron. Soc.,* **476**, 1310—1330. DOI: 10.1093/mnras/sty204
30. Martins J. V. (2018). *The Hyperangular Imaging Polarimeter (HARP) and the Use of Nanosatellites for Earth Science Remote Sensing*. URL: http://www.fap.if.usp.br/~hbarbosa/uploads/Site/ JournalClub/Vanderlei_11jul2018.pdf (Last accessed: 23.02.2024).
31. McKee C., Ostriker E. (2007). Theory of Star Formation. *Annu. Rev. Astron. and Astrophys.*, **45**, 565—687. DOI: 10.1146/annurev.astro.45.051806.110602.
32. Milinevsky G., Oberemok Y., Syniavskyi I., Bovchaliuk A., Kolomiets I., Fesianov I., Wang Y. (2019). Calibration model of polarimeters on board the Aerosol-UA space mission. *J. Quant. Spectrosc. and Radiat. Transfer.*, **229**(5), 92—105. DOI: 10.1016/j.jqsrt.2019.03.007
33. Minami Y. (2020). Determination of miscalibrated polarization angles from observed cosmic microwave background and foreground EB power spectra: Application to partial-sky observation. *Prog. Theor. Exp. Phys.*, **6**, 063E01. DOI: 10.1093/ptep/ptaa057
34. Minami Y., Komatsu E. (2020). New Extraction of the Cosmic Birefringence from the Planck 2018 Polarization Data. *Phys. Rev. Lett.*, **125**, 221301. DOI: 10.1103/PhysRevLett.125.221301.
35. Minami Y., Ochi H., Ichiki K., Katayama N., Komatsu E., Matsumura T. (2019). Simultaneous determination of the cosmic birefringence and miscalibrated polarization angles from CMB experiments. *Prog. Theor. Exp. Phys.*, **2019**(8), 083E02. DOI: 10.1093/ptep/ptz079.
36. Mudge J., Virgen M., Dean P. (2009). Near-infrared simultaneous Stokes imaging polarimeter. *Proc. SPIE*, **7461**, 74610L-1—74610L-6. DOI: 10.1117/12.828437
37. Mu T., Bao D., Han F., Sun Y., Chen Z., Tang Q., Zhang C. (2019). Optimized design, calibration, and validation of an achromatic snapshot full-Stokes imaging polarimeter. *Opt. Express*, **27**(16), 23009—23028. DOI: 10.1364/OE.27.023009.
38. Mu T., Zhang C., Liang R. (2015). Demonstration of a snapshot full-Stokes division-of-aperture imaging polarimeter using Wollaston prism array. *J. Opt.*, **17**(12), 125708. DOI: 10.1088/2040-8978/17/12/125708
39. Mu T., Zhang C., Li Q., Liang R. (2015). Error analysis of single-snapshot full-Stokes division-of-aperture imaging polarimeters. *Opt. Express*, **23**(8), 10822—10835. DOI: 10.1364/OE.23.010822.

40. Oliva E. (1997). Wedged double Wollaston, a device for single shot polarimetric measurements. *Astron. and Astrophys. Suppl. Ser.*, **123**(3), 589—592. DOI: 10.1051/aas:1997175.
41. Pedersini F., Sarti A., Tubaro S. (1999). Accurate and simple geometric calibration of multi-camera Systems. *Signal Proc.*, **77**(3), 309—334. DOI: 10.1016/S0165-1684(99)00042-0
42. Pernechele C., Abe L., Bendjoya P., Cellino A., Massone G., Rivet J. P., Tanga P. (2012). A "single-shot" optical linear polarimeter for asteroids studies. *Proc. SPIE*, **8446**, 84462H-1-6. DOI: 10.1117/12.925933
43. Perreault J. D. (2013). Triple Wollaston-prism complete-Stokes imaging polarimeter. *Opt. Lett.*, 38(19), 3874—3877. DOI: 10.1364/OL.38.003874.
44. Pezzaniti J. L., Chenault D., Roche M., Reinhardt J., Pezzaniti J. P., Schultz H. (2008). Four camera complete Stokes imaging polarimeter. *Proc. SPIE.*, **6972**, 69720J-1b—69720J-12. DOI: 10.1117/12.784797.
45. Piran T. (1999). Gamma ray bursts and the fireball model. *Phys. Rep.*, **314**(6), 575—667. DOI: 10.1016/S0370-1573(98)00127-6.
46. Radecke H. D., Kanbach G. (1992). The Egret High Energy Gamma Ray Telescope on GRO: Instrument Description and Scientific Mission. *Data Analysis in Astronomy IV*. Ed. V. Di. Gesu et al., 303—310. DOI: 10.1007/978-1-4615-3388-7_31.
47. Ramaprakash A. N., Rajarshi C. V., Das H. K., Khodade P., Modi D., Panopoulou G., Maharana S., Blinov D., Angelakis E., Casadio C., Fuhrmann L., Hovatta T., Kiehlmann S., King O. G., Kylafis N., Kougentakis A., Kus A., Mahabal A., Marecki A., Myserlis I., Paterakis G., Paleologou E., Liodakis I., Papadakis I., Papamastorakis I., Pavlidou V., Pazderski E., Pearson T. J., Readhead A. C. S., Reig P., Slowikowska A., Tassis K., Zensus J. A. (2019). RoboPol: A four-channel optical imaging polarimeter. *Mon. Notic. Roy. Astron. Soc.*, **485**, 2355—2366. DOI: 10.1093/mnras/stz557.
48. Romero G. (2005). Proc. Marcel Grossmann 10th Meeting, World Scientific Publishing (Singapore), P. 2429.
49. Shestopalov D. I., Golubeva L. F. (2015). Polarimetric properties of asteroids. *Adv. Space Res.*, **56**, 2254—2274. DOI: 10.1016/j.asr.2015.08.013
50. Shibata S., Hagen N., Kawabata S., Otani Y. (2019). Compact and high-speed Stokes polarimeter using three-way polarization-preserving beam splitters. Appl. Opt., **58**(21), 5644—5649. DOI: 10.1364/AO.58.005644
51. Shrestha M., Steele I. A., Piascik A. S., Jermak H., Smith R. J., Copperwheat C. M. (2020). Characterization of a dual-beam, dual-camera optical imaging polarimeter. *Mon. Notic. Roy. Astron. Soc.,* **494**, 4676—4686. DOI: 10.1093/mnras/staa1049
52. Shu F., Adams F., Lizano S. (1987). Star Formation in Molecular Clouds: Observation and Theory. *Annu. Rev. Astron. and Astrophys.*, **25**, 23—81. DOI: 10.1146/annurev.aa.25.090187.000323
53. Sillanpää A., Takalo L. O., Nilsson K., Kikuchi S. (1993). Photopolarimetry of BL Lac. *Astrophys. Space Sci.,* **206**, 55—70. DOI: 10.1007/BF00658383.
54. Sinyavskiĭ I. I., Ivanov Yu. S., Vid'machenko A. P. (2013). Concept of the construction of the optical setup of a panoramic Stokes polarimeter for small telescopes. *J. Opt. Technol.*, **80**(9), 545—548. DOI: 10.1364/JOT.80.000545.
55. Steele I. A., Mundell C. G., Smith R. J., Kobayashi S., Guidorzi C. (2009). Ten percent polarized optical emission from GRB-090102. *Nature*, **462**, 767—769. DOI: 10.1038/nature08590
56. Svalheim T. L., Andersen K. J., Aurlien R., Banerji R., Bersanelli M., Bertocco S., Brilenkov M., Carbone M., Colombo L. P. L., Eriksen H. K., Foss M. K., Franceschet C., Fuskeland U., Galeotta S., Galloway M., Gerakakis S., Gjerløw E., Hensley B., Herman D., Iacobellis M., Ieronymaki M., Ihle H. T., Jewell J. B., Karakci A., Keihänen E., Keskitalo R., Maggio G., Maino D., Maris M., Paradiso S., Partridge B., Reinecke M., Suur-Uski A.-S., Tavagnacco D., Thommesen H., Watts D. J., Wehus I. K., Zacchei A. (2023). Beyond Planck. XIV. Polarized foreground emission between 30 and 70 GHz. *Astron. and Astrophys.*, **675**, A14. DOI: 10.1051/0004-6361/202243160.
57. Syniavskyi I., Ivanov Yu. S. (2014). Four-channel imaging Stokes polarimeter for small telescopes. *Contrib. Astron. Observ. Skalnate Pleso*, **43**, 253—255.
58. Syniavskyi I. I., Ivanov Yu. S., Sosonkin M. G., Milinevsky G. P., Koshman G. (2018). Multispectral imager-polarimeter of the "AEROSOL-UA" space project. *Space Sci. and Technol.*, **24**(3), 23—32. DOI: 10.15407/knit2018.03.023.
59. Syniavskyi I., Oberemok Ye., Danylevsky V., Bovchaliuk A., Fesianov I., Milinevsky G., Savenkov S., Yukhymchuk Yu., Sosonkin M., Ivanov Yu. (2021). Aerosol-UA satellite mission for the polarimetric study of aerosols in the atmosphere. *J. Quant. Spectrosc. and Radiat. Transfer.*, **267**, 107601. DOI: 10.1016/j.jqsrt.2021.107601
60. Tedesco E. F. (1994). Asteroid albedos and diameters. *Asteroids, comets, meteors 1993:* Proc. 160th Int. Astron. Union (Belgirate, Italy, June 14—18, 1993). Eds A. Milani, M. Di Martino, and A. Cellino. *Int. Astron. Union. Symp.,* No. 160*,* 55—74.
61. Toth L. V., Doi Y., Zahorecz S., Pinter S., Racz I. I., Bagoly Z., Balazs L.G., Horvath I., Kiss C., Kovács T., Onishi T. (2019). Galactic foreground of gamma-ray bursts from AKARI Far-Infrared Surveyor. *Publ. Astron. Soc. Jap.,* **71**(1), 10 (1—20). DOI: 10.1093/pasj/psy123.
62. Tyo J., S., Goldstein D., L., Chenault D. B., Shaw J. A. (2006). Review of passive imaging polarimetry for remote sensing applications. *Appl. Opt.*, **45**(22), 5453—5469. DOI: 10.1364/AO.45.005453.

63. Zhang H. (2019). Blazar optical polarimetry: Current progress in observations and theories. *Galaxies*, **7**(4)**,** 85. DOI: 10.3390/galaxies7040085.
64. Zhang Z. (2020). A flexible new technique for camera calibration. *IEEE Transactions on Pattern Analysis and Machine Intelligence*, **22**, 1330—1334. DOI: 10.1109/34.888718.
65. Zhu S., Jin S., Shu Y., Liu Z., Hong J. (2023) Polarization calibration method for simultaneous imaging polarization camera. *Proc. SPIE.,* **125570D**. DOI: 10.1117/12.2646131

Стаття надійшладо редакції 02.02.2024 *Received 02.02.2024*
Після доопрацювання 18.03.2024 *Revised 18.03.2024*
Прийнято до друку 18.03.2024 *Accepted 18.03.2024*

І. І. Синявський[1], зав. відділу, канд. техн. наук, старш. дослідник
А. Кастро-Тірадо[2], професор, PhD
Ю. С. Іванов[1], старш. наук. співроб.
С. С. Гузій[2,3], наук. співроб.[2], доцент[3], канд. фіз.-мат. наук
Є. А. Оберемок[1,4], наук. співроб.[1], доцент[4], канд. фіз.-мат. наук

[1] Головна астрономічна обсерваторія Національної академії наук України
вул. Академіка Заболотного 27, Київ, Україна, 03143
[2] Інститут астрофізики Андалусії
Glorieta de la Astronomía s/n, 18008, Гранада, Іспанія
[3] Чорноморський національний університет ім. Петра Могили
вул. 68 Десантників 10, Миколаїв, Україна, 54000
[4] Київський національний університет імені Тараса Шевченка
вул. Володимирська 60, Київ, Україна, 01033

ШИРОКОКУТНИЙ СТОКС-ПОЛЯРИМЕТР ДЛЯ МЕРЕЖІ ТЕЛЕСКОПІВ BOOTES. ОПТИЧНИЙ ТА МЕХАНІЧНИЙ ДИЗАЙН

Розглянуто зображувальний поляриметр EDIPO (Efficient & Dedicated wide-field Imaging Polarimeter), який у комбінації з астрономічними телескопами мережі BOOTES (Burst Observer and Optical Transient Exploring System) призначений для дослідження поляризаційних особливостей швидкоплинних процесів післясвітіння гамма-спалахів (Gamma-ray burst — GRB). Конструкція поляриметра дозволяє встановлювати його на телескопи мережі з діаметром головного дзеркала до 1.4 м. Поляриметр спроєктовано для проведення аналізу параметрів поляризації повністю та частково лінійно поляризованого випромінювання у спектральному діапазоні 450 —1000 нм. Аналізатор поляризації не містить рухомих елементів і дозволяє проводити вимірювання параметрів Стокса I, Q, U випромінювання у полі зору 30' × 30' одномоментно для однієї спектральної смуги робочого спектрального діапазону. Оптичну частину поляриметра без спектральних фільтрів та аналізатора поляризації виготовлено, зібрано та випробувано на телескопі з діаметром дзеркала 1.23 м. Розглянуто можливі підходи до поляриметричного калібрування системи поляриметр —телескоп.

***Ключові слова*:** поляризація, Стокс-поляриметр, телескоп.